ELSEVIER

Journal of Biomechanics 35 (2002) 813–821

JOURNAL OF BIOMECHANICS

www.elsevier.com/locate/jbiomech
www.JBiomech.com

# Hydrodynamics of magnetic drug targeting

P.A. Voltairas[a,*], D.I. Fotiadis[a], L.K. Michalis[b]

[a] Department of Computer Science, University of Ioannina, Ioannina 451 10, Greece
[b] Department of Cardiology, Medical School, University of Ioannina, Ioannina 451 10, Greece

Accepted 5 February 2002

**Abstract**

Among the proposed techniques for delivering drugs to specific locations within the human body, magnetic drug targeting surpasses due to its non-invasive character and its high targeting efficiency. Although the method has been proposed almost 30 years ago, the technical problems obstruct possible applications. It is the aim of the present work to classify the emerging problems and propose satisfactory answers. A general phenomenological theory is developed and a model case is studied, which incorporates all the physical parameters of the problem. © 2002 Elsevier Science Ltd. All rights reserved.

*Keywords:* Biomaterials; Biorheology; Ferrofluids; Magnetic drug targeting; Thrombosis

## 1. Introduction

Magnetism is one of the major contributors in biological and biomedical research (Adrä and Nowak, 1998). Among the many applications of magnetic carriers we mention some recent ones, such as the use of magnetic microbeads in DNA array biosensors (Miller et al., 2001), magnetic elastomers in otiatria as a biomimetic prosthetic tympanic membrane (Kuznetsov et al., 2001) and ferrofluid internal tamponade in retinal detachment surgery (Voltairas et al., 2001). Magnetite nanoparticles have been detected recently in the human hippocampus (Schultheiss-Grassi et al., 1999). and can shed some light to the process of iron biomineralization. Also the biological and neurophysiological effects of magnetic fields is the subject of a big controversy (Voustianiouk and Kaufmann, 2000).

The concept of magnetic drug targeting is not new (Mosbach and Schröder, 1979). Efficient drug targeting is vital for the medical treatment of various diseases and among them of cardiovascular episodes, like stenosis and thrombosis. Ferrofluids, magnetoliposomes and magnetic micro and nanospheres are promising candidates, for delivering drugs to specific locations within the body, with high accuracy, minimum or no surgical intervention and maximum concentration. Their building blocks, the ferromagnetic particles, with the permanent magnetic polarization and the magnetophoretic mobility that they develop in an applied magnetic field, are responsible for their improved properties. The ternary phase structure of blood (white–red blood cells and plasma), as well as the plethora of particles that are present in the blood flow, makes hemodynamics an exceedingly complex research field. Visualization of complex flow patterns in the heart has been accomplished recently, through combined MRI and computational imaging techniques (Kilner et al., 2000). Moreover, the response of blood in magnetic fields in not yet completely known, though there are some indications for the diamagnetic, paramagnetic, or ferromagnetic character of its various constituents (Higashi et al., 1997; Iwasaka et al., 1994a,b; Haik et al., 2001).

The thrombolytic properties of high magnetic fields is also an open field of investigation (Iwasaka et al., 1994a, b; Iwasaka et al., 1996; Iwasaka et al., 1998). In arteriosclerosis episodes, like stenosis and thrombosis, what is important is to keep the thrombolytic drug, usually aspirin, in contact with the source of the problem, the endothelial cells, which are located along the inner wall of the blood vessel. Some in-vitro and in-vivo experiments have been performed in this direction (Rusetski and Ruuge, 1990; Ruuge and Rusetski, 1993; Torchilin, 2000). Nevertheless, firm theoretical foundation of magnetic drug targeting is still lacking.

Provided that the biocompatibility of magnetic particles will be accomplished, investigation of the

*Corresponding author. Tel.: +30-651-98821; fax: +30-651-98889.
*E-mail address:* pvolter@cs.uoi.gr (P.A. Voltairas).


PII: S0021-9290(02)00034-9

conditions, for holding a ferrofluid drop on a blood vessel wall, is required. For that purpose, a self-consistent ferrohydrodynamic theory of magnetic drug targeting is presented and a model case is examined, to account for adhesion. The physical complexity, though it is not avoided, is kept to the minimum. Technical problems, concerning the design and the focusing of the strength of the externally applied non-uniform magnetic field, along the blood vessel wall, are stressed. We obtain an upper bound of the mean blood flow velocity as a function of the applied magnetic field, which permits quantitative estimation of the adherence condition. Comparison between the theoretically calculated and the experimentally observed blood velocity, for the carotid artery (Perret and Sloop, 2000), confirm the presence of the upper bound, for given magnetic field strength, blood and magnetic drug viscosity and geometrical parameters of the model.

## 2. Ferrohydrodynamic formulation

### 2.1. General theory

In order to define conditions for adhesion of a magnetic fluid (ferrofluid) drug on a blood vessel wall, we encounter a highly complex situation, where we have to incorporate magnetostatic field effects on two phase (ferrofluid–blood) flow. Scrutiny requires taking also into account the effects of static magnetic fields on blood flow. The knowledge of the biological effects of static or dynamic electromagnetic fields is still in its infancy. The response of blood on static magnetic fields depends on a variety of factors like: oxygen content, pH, temperature gradients, etc. Thus, for example, plasma and leucocytes (like in most biological tissues) are under normal conditions diamagnetic, while oxy- and deoxygenated erythrocytes are dia- and paramagnetic, respectively (Higashi et al., 1997). One might expect that since hemoglobin, the basic molecule that constitutes erythrocytes, contains an iron atom as a core, should be ferromagnetic, but it is its overall structure that results in the observed dia- or paramagnetic character. Thus, conditions that will determine the strength of the external static magnetic field and the magnetic density of the ferrofluidic drug, for adherence, must be optimized in order to avoid possible side effects on the blood flow.

Although the exact rules that govern the physiology of blood circulation are still unknown, due to the diversity of the blood constituents and the complexity of the vascular system (Fung, 1997), we will assume that classical continuum hydrodynamical conservation laws are applicable. Thus according to the general theory of hydrodynamics, the blood and the magnetic drug flow are described by the conservation of momentum, or Navier–Stokes equations of fluid motion, in the absence of temperature gradients, augmented for the case of the magnetic drug with a magnetic body force term $\tau^{\mathrm{M}}_{ij,j}$ (Rosensweig, 1997):

$$\tau_{ij,j} + \tau^{\mathrm{M}}_{ij,j} + f_i = \rho\left(\frac{\partial u_i}{\partial t} + u_k\, u_{i,k}\right), \tag{1}$$

where

$$\tau_{ij} = -p\,\delta_{ij} + \eta\,(u_{i,j} + u_{j,i}), \tag{2}$$

$$\tau^{\mathrm{M}}_{ij} = H_i B_j - \mu_0\left(\frac{H_k H_k}{2} + \int_0^H \frac{\partial(\upsilon M)}{\partial \upsilon}\,\mathrm{d}H\right)\delta_{ij}, \tag{3}$$

$$B_i = \mu_0(H_i + M_i) \tag{4}$$

and by the conservation of mass:

$$\frac{\partial \rho}{\partial t} + \nabla\cdot(\rho \boldsymbol{u}) = 0. \tag{5}$$

Here, $\tau_{ij}$ is the stress tensor, $\tau^{\mathrm{M}}_{ij}$ is the Maxwell stress tensor, $f_i$ is the body force term, $\rho$ is the density of the fluid, $u_i$ is the velocity, $p$ is the pressure, $\eta$ is the viscosity, $B_i$ is the magnetic induction, $H_i$ is the magnetic field, $M_i$ is the magnetization, $\upsilon = 1/\rho$ is the specific volume, $\mu_0$ is the magnetic permeability of vacuum and $\delta_{ij}$ is the Kronecker delta. $H_i = H'_i + H^0_i$ is the total magnetic field due to external $H^0_i$, and internal $H'_i$ origin. $H'_i$ is usually known as the demagnetizing field produced by volume $\nabla\cdot\boldsymbol{M}$ or surface $\hat{\boldsymbol{n}}\cdot\boldsymbol{M}$ magnetic charges, where $\hat{\boldsymbol{n}}$ is the unit outward vector. The Einstein's summation convention is adopted with $(\,)_{,i} \equiv \partial/\partial x_i$, and bold characters denote vector fields. In general it must be added to the Maxwell stress tensor (3) a term due to the non-collinearity of the magnetic field with the magnetization, proportional to $\boldsymbol{M}\times\boldsymbol{H}$. In the following we assume a magnetization collinear with the applied magnetic field ($M_i = \chi H_i$, $\chi$ is the magnetic susceptibility), thus such a term can be neglected. To the equations of fluid motion (1) the magnetostatic field equations must be added:

$$\nabla\cdot\boldsymbol{B} = 0, \tag{6}$$

$$\nabla\times\boldsymbol{H} = 0. \tag{7}$$

From hereafter the subscripts $(\,)_1$ and $(\,)_2$ will denote quantities of the magnetic drug and blood regions, respectively. The formulation of the initial boundary value problem (IBVP) (1), (5)–(7) is completed with the appropriate initial and boundary conditions. The initial conditions for a pulsating fluid flow are

$$\boldsymbol{u}_i(t = t_0, \boldsymbol{r}) = \mathbf{v}_i(\boldsymbol{r}), \quad i = 1, 2. \tag{8}$$

We have two boundary surfaces $S_k$, $k = 1, 2$, where $k = 1$ corresponds to magnetic drug–blood interface, and $k = 2$ to the blood vessel wall. When the magnetic drug is in contact with the blood vessel wall (also known as endothelium) we have to consider also another interface $S_3$ (Fig. 1(b)). On the interface $S_1$ the boundary

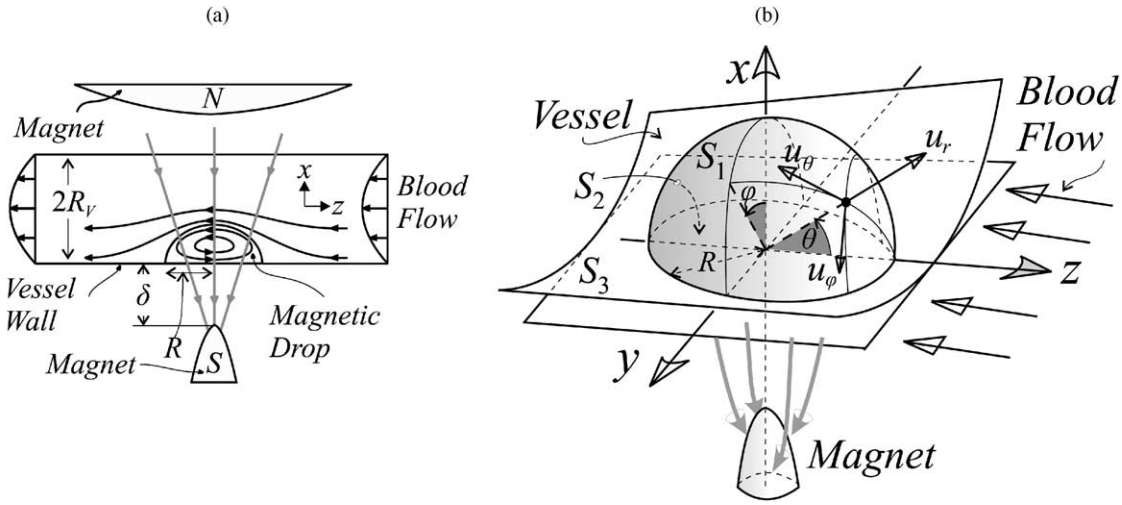


Fig. 1. Model geometry. (a) Cross-section along the $zx$-plane. (b) Coordinate system.

conditions for the hydrodynamic problem (1) are

$$\hat{\boldsymbol{n}} \cdot \boldsymbol{u}_1 = \hat{\boldsymbol{n}} \cdot \boldsymbol{u}_2 = 0, \tag{9}$$

$$\hat{\boldsymbol{n}} \times [\![ \boldsymbol{u} ]\!] = 0, \tag{10}$$

$$[\![ \tau_{ij} + \tau_{ij}^{\mathrm{M}} ]\!] \, \hat{n}_i \, \hat{n}_j = \gamma \, n_{i,i}, \tag{11}$$

$$[\![ \tau_{ij} + \tau_{ij}^{\mathrm{M}} ]\!] \, \hat{n}_i \, \hat{t}_j = 0, \tag{12}$$

where $\gamma$ is the surface tension, $\hat{\boldsymbol{t}}$ is tangential unit vector, and for the magnetic potential problem (5)–(6) are

$$\hat{\boldsymbol{n}} \cdot [\![ \boldsymbol{B} ]\!] = 0, \tag{13}$$

$$\hat{\boldsymbol{n}} \times [\![ \boldsymbol{H} ]\!] = 0. \tag{14}$$

The abbreviation $[\![ A ]\!] = A_2 - A_1$ is used in the boundary conditions (9)–(14). The BCs (9)–(12) correspond to the vanishing of the normal velocity components, to the continuity of the tangential velocity components, to the jump of the normal surface tractions and to the continuity of the tangential surface tractions, respectively, while the BCs (13)–(14) are the usual ones, for the magnetostatic potential problem (6)–(7). The no slip conditions for the velocity field on the interfaces $S_k$, $k = 2, 3$ read:

$$\boldsymbol{u}_i = 0, \quad i = 1, 2. \tag{15}$$

In a general pulsating flow the interfaces $S_k$, $k = 2, 3$ are not rigid but deform in an elastic or viscoelastic manner. Finally, the finiteness of the flow at the origin and at infinity requires:

$$\boldsymbol{u}_1(t, \boldsymbol{r} \to 0) = \boldsymbol{u}_0, \tag{16}$$

$$\boldsymbol{u}_2(t, \boldsymbol{r} \to \infty) = \boldsymbol{u}_\infty. \tag{17}$$

Similar conditions are necessary for the magnetic field $\boldsymbol{H}$ as well. The above developed IBVP has to be solved for the velocity field $\boldsymbol{u}(t, \boldsymbol{r})$, for given magnetic field configuration $\boldsymbol{H}(\boldsymbol{r})$. In the general case, the apparent difficulties are enormous, and so some special problems will be discussed below.

## 3. The model

In order to appreciate on the difficulties that we encounter in the solution, we just mention that even in oversimplified cases where the hydrodynamic problem (1) is neglected and one faces the solution of the magnetostatic potential problem (6)–(7) and the free boundary condition (11), results are obtained only with properly designed finite element codes using supercomputers (Boudouvis and Scriven, 1993; Papathanasiou and Boudouvis, 1999). For that purpose a qualitative analysis will be presented, with emphasis on the responsible physical mechanisms for adherence, like the strength of the magnetic field and the magnetization of the ferrofluidic drug that overcomes the blood velocity. Well known analytical results will be combined to account for the hydrodynamic drag exerted by the blood flow on the ferrofluidic drop and for the magnetophoretic driving force and its limitations. A more elaborated investigation, with the development of a numerical model, that will satisfy the full IBVP, described above, will be the subject of future investigations.

We assume that the magnetic drug constitutes a hemisphere like structure of radius $R$ attached to the blood vessel wall, with the coordinate origin located on the center of the primitive circle on the equatorial plane of the hemispherical drop (Fig. 1(a) and (b)). Diffusion phenomena are neglected ($\rho_1 = \rho_2$). The blood vessel is considered to be an infinite, rectilinear, rigid, nonporous cylindrical tube, with smooth internal surface, of radius $R_V$. We will address the case $R_V \gg R$, in order for the equatorial plane of the hemispherical drop to

coincide with the blood vessel wall. The ferrofluidic drug will originally be supplied through a catheter in the blood stream, thus it is more likely to have a prolate hemispheroidal like shape, but for computational convenience we investigate here a hemispherical like drop. The extension is straight forward for the prolate case and will be discussed in a future work. Moreover, adhesion effects, due to Van der Walls forces, possible lift effects on the drug–vessel wall interface and buoyancy forces will be neglected because of the strength of the magnetophoretic force. In order to simplify further the magnetic potential problem, we consider a diluted, incompressible ferrofluidic drug, with no temperature gradients. The first two of the above simplifications are justified, since we usually need water based drugs to avoid side effects. As far as the absence of temperature gradient effects is concerned, this is acceptable for local flow considerations. Then the third term of the Maxwell stress tensor of Eq. (3) will be omitted, the magnetization depends only on the external field ($\boldsymbol{H} \approx \boldsymbol{H}^0$), and the magnetic body force terms in the equation of fluid motion (1) vanishes. We will limit our discussion on the low Reynolds number regime, where inertial effects are neglected. This is a legitimate approximation for capillaries and thin vessels, or for possible slow viscous flows in larger vessels. Then the equations of motion (1) and the equation of continuity (5), reduce to the Stokes flow for the velocity field $\boldsymbol{u}$:

$$\eta \nabla^2 \boldsymbol{u} = \nabla p, \tag{18}$$

$$\nabla \cdot \boldsymbol{u} = 0 \tag{19}$$

and the magnetostatic potential problem (6)–(7) is neglected. Similarly, due to the above assumptions the boundary conditions (11)–(12) are rewritten as

$$[\![ p_{vn} - p ]\!] + p_m + p_n = p_c, \tag{20}$$

$$[\![ p_{vt} ]\!] = 0, \tag{21}$$

where

$$p_{vn} = 2\eta\, \hat{\boldsymbol{n}} \cdot \frac{\partial \boldsymbol{u}}{\partial \hat{n}}, \tag{22}$$

$$p_{vt} = \eta \left( \hat{\boldsymbol{t}} \cdot \frac{\partial \boldsymbol{u}}{\partial \hat{n}} + \hat{\boldsymbol{n}} \cdot \frac{\partial \boldsymbol{u}}{\partial \hat{t}} \right) \tag{23}$$

are the normal and tangential viscous pressures on the interface $S_1$, respectively, with $\partial/\partial \hat{n} \equiv \hat{\boldsymbol{n}} \cdot \nabla$, $\partial/\partial \hat{t} \equiv \hat{\boldsymbol{t}} \cdot \nabla$, and $p_m$, $p_n$ and $p_c$ have the usual notations as in Rosensweig (1997):

$$p_m = \mu_0 \int_0^H M \, \mathrm{d}H = \mu_0 \int_0^H \chi\, H \, \mathrm{d}H, \tag{24}$$

$$p_n = \frac{\mu_0 M_n^2}{2} = \frac{\mu_0 \chi^2 H_n^2}{2}, \tag{25}$$

$$p_c = \gamma \nabla \cdot \hat{\boldsymbol{n}} \tag{26}$$

with $H_n = \hat{\boldsymbol{n}} \cdot \boldsymbol{H}$ and $H_t = \hat{\boldsymbol{t}} \cdot \boldsymbol{H}$. In general, the constitutive law $M = \chi H$ might be non-linear ($\chi = \chi(H)$), but in the following we will limit ourselves to a linear constitutive law ($\chi = \text{const.}$). Notice the absence of magnetic pressure terms in Eq. (18). By considering for the moment axisymmetric solutions of the form

$$\boldsymbol{u} = \nabla \times \left( \frac{\Psi(r,\theta)}{r \sin\theta} \hat{\boldsymbol{e}}_\phi \right), \tag{27}$$

which fulfill condition Eq. (19), and by taking the curl of Eq. (18) this reduces to the following PDE for the stream function $\Psi$:

$$\left[ \frac{\partial^2}{\partial r^2} + \frac{\sin\theta}{r^2} \frac{\partial}{\partial \theta} \left( \frac{1}{\sin\theta} \frac{\partial}{\partial \theta} \right) \right]^2 \Psi = 0. \tag{28}$$

Following separation of variables of the form $\Psi = r^n \sin^k \theta$, and considering only the $k = 2$ mode, the permissible $n$'s are $n = -1, 2, 3, 4$ thus:

$$\Psi = \left( \frac{C_1}{r} + C_2 r + C_3 r^2 + C_4 r^4 \right) \frac{\sin^2 \theta}{2}. \tag{29}$$

The constants in Eq. (29) are determined from the BCs (9)–(10), (12), (16)–(17) with

$$\boldsymbol{u}_\infty = -\boldsymbol{u}_0 = -u_0 \hat{\boldsymbol{e}}_z, \quad (u_0 > 0) \tag{30}$$

and $\hat{\boldsymbol{e}}_z = \cos\theta \hat{\boldsymbol{e}}_r - \sin\theta \hat{\boldsymbol{e}}_\theta$. Then the flows in regions (1) and (2) become

$$\boldsymbol{u}_1 = \lambda_3 u_0 \left[ \left( 1 - \left( \frac{r}{R} \right)^2 \right) \cos\theta\, \hat{\boldsymbol{e}}_r - \left( 1 - 2 \left( \frac{r}{R} \right)^2 \right) \sin\theta\, \hat{\boldsymbol{e}}_\theta \right], \tag{31}$$

$$\boldsymbol{u}_2 = u_0 \left\{ \left[ 2\lambda_1 \left( \frac{R}{r} \right) - 2\lambda_2 \left( \frac{R}{r} \right)^3 - 1 \right] \cos\theta\, \hat{\boldsymbol{e}}_r - \left[ \lambda_1 \left( \frac{R}{r} \right) + \lambda_2 \left( \frac{R}{r} \right)^3 - 1 \right] \sin\theta\, \hat{\boldsymbol{e}}_\theta \right\} \tag{32}$$

with

$$\lambda_1 = \frac{2\eta_2 + 3\eta_1}{4(\eta_1 + \eta_2)}, \quad \lambda_2 = \frac{\eta_1}{4(\eta_2 + \eta_1)}, \quad \lambda_3 = \frac{\eta_2}{2(\eta_1 + \eta_2)}. \tag{33}$$

Substitution of (31)–(32) into (18) and integration deduces the pressures

$$p_1 = 5\eta_1 \lambda_3 u_0 r \frac{\cos\theta}{R^2}, \tag{34}$$

$$p_2 = 2\eta_2 \lambda_1 u_0 R \frac{\cos\theta}{r^2}. \tag{35}$$

The solution (31)–(32) does not satisfy the no slip conditions (15). An efficient way to overcome this problem is to search for surfaces where two different flows coincide, and each one of the flows satisfy the appropriate boundary conditions in the region separated by the surface. This is permissible due to the linearity of

the problem. Thus, for example, one such surface for the two flows $\boldsymbol{u}_{\text{up}}$ and $\boldsymbol{u}_{\text{down}}$ is the following:

$$(\boldsymbol{u}_{\text{up}} - \boldsymbol{u}_{\text{down}})^2 = 0. \tag{36}$$

In order to determine flows that satisfy the no slip conditions (15), we searched for asymmetric flows of the form (27) with $\Psi = \Psi(r, \theta, \phi)$ and no singularities inside the hemispherical drop, by the method of separation of variables. The only acceptable non-singular solution was the usual shear flow

$$\boldsymbol{u}_s = u_s x \hat{\boldsymbol{e}}_z. \tag{37}$$

Far away from the drop it is legitimate to assume that the flow is of the Poiseuille type

$$\boldsymbol{u}_p = u_p(r, \theta, \phi)(\cos\theta\, \hat{\boldsymbol{e}}_r - \sin\theta \hat{\boldsymbol{e}}_\theta) \tag{38}$$

with

$$u_p(r, \theta, \phi) = -u_0 \left[ \left(\frac{r}{R}\right)^2 \sin^2\theta - 2\left(\frac{r}{R}\right) \sin\theta \cos\phi \right]. \tag{39}$$

Looking for a surface of the form (36) inside the magnetic drop, with $\boldsymbol{u}_{\text{up}} = \boldsymbol{u}^{(1)}$ and $\boldsymbol{u}_{\text{down}} = \boldsymbol{u}_s$ we deduce that such a surface has a maximum at $x_m/R = (-\alpha \pm \sqrt{\alpha^2 + 8})/4$, $y = z = 0$, $\alpha = u_s/(\lambda_1 u_0)$, and intersects the equatorial plane $x = 0$, along a closed elliptic like curve with $z = \pm R$ and $y = \pm R/\sqrt{2} \approx \pm 0.7R$, which is not far from the primitive circle $r = R$. Notice that $0 \leqslant x_m/R \leqslant 1$ for $\alpha > 0$ and $\alpha \to 0$. Thus, for the qualitative estimations presented here, the shear flow presented above is a sufficient approximation for the flow inside the drop and close to the blood vessel wall (equivalent results are obtained if we use, instead of a shear, a Poiseuille type flow). Following a similar procedure for the determination of surfaces that separate modified Poiseuille or shear flows outside the drop, we obtained acceptable results only for the space in front of the drop with respect to the direction of the blood velocity, but not behind. Nevertheless, despite the inconsistencies on the satisfaction of the no slip conditions (15) inside and outside the ferrofluidic drop, we will assume that the flow (31)–(32) is appropriate for our qualitative computations. In a more accurate calculation, it is expected that due to the no slip condition, the drag that experiences the magnetic drop will be a bit smaller from the one obtained from Eqs. (31)–(32).

## 4. The adhesion condition

Even if we will derive a flow that satisfies the BCs (15) we have also to fulfill the BC (20) on the free boundary $S_1$, that determines the type of deformation of the magnetic drop in the presence of the blood flow. Our primary concern here is to estimate under what conditions the magnetic drop adheres to the blood vessel wall. In order to keep the mathematics simple without loosing the physical understanding, we might assume that the shape of the drop remains unaltered (hemispherical). Then we have to replace the capillary pressure (26) by the equivalent for the sphere

$$p_c = \frac{2\gamma}{R}. \tag{40}$$

With the substitution of Eq. (40) into (20) the later defines the stability boundary against decomposition into smaller drops, and thus it may be considered as a suitable adhesion condition. But even then we have to introduce an adapted inhomogeneous magnetic field, that will counteract to the blood flow, in order for the condition (20) to result in an expression for the mean blood velocity as a function of the maximum external field. For our problem geometry a legitimate form of the external magnetic field, would be in a first approximation that produced by a point source located outside the body at $x = -\delta$, $y = 0$, $z = \zeta$, $(\delta, \zeta > 0)$, (see Fig. 2(b)), of the form

$$\boldsymbol{H} = \frac{m(\boldsymbol{r} + \delta \hat{\boldsymbol{e}}_x - \zeta \hat{\boldsymbol{e}}_z)}{(r^2 + \delta^2 + \zeta^2 + 2\delta x - 2\zeta z)^{3/2}} \tag{41}$$

on the reference frame attached to the magnetic drop, with $m$ the magnetic dipole moment. This is a typical Coulomb field. A dipole source would also be a sufficient approximation, but we adopt the form (41) since it approximates well conical magnetic spikes designs, of a biomedical apparatus. It has to be emphasized here that the non-uniformity of the applied magnetic field, which is vital for the magnetophoretic mobility of the ferrofluid drug, is higher only close to the magnetic pole. This is a major technical problem that has to be resolved, in order for the drug targeting to remain essentially non-invasive. This limitation in bulk vessels is not present on surface ones. Semi-invasive techniques, like magnetic needles, provide always an alternative solution. The fact that the magnetic point source is oriented at an angle

$$\omega = \arcsin\left(\frac{\zeta}{\delta}\right) \tag{42}$$

with respect to the $x$-axis of our coordinate system (see Fig. 2(b)) will be apparent from the following discussion. The boundary condition (11) or (20) can also be rewritten in vectorial form as

$$[\![\, \boldsymbol{T} \,]\!] = p_c \hat{\boldsymbol{n}}, \quad T_i = (\tau_{ij} + \tau_{ij}^{\text{M}}) n_j. \tag{43}$$

Substitution of (31)–(32) and (40)–(41) into (20) results in an expression that contains not similar azimuthal and polar components, which cannot be satisfied. In order to overcome this obstacle we might replace the local condition (20) by the more global one after integrating (20) over the surface area $S_1$, which written in

dimensionless form, reads

$$\frac{1}{B_m} = \frac{\chi}{4S_0} \int\int_{S_1} (h^2 + h_n^2)\, \mathrm{d}S, \tag{44}$$

where

$$B_m = \frac{\mu_0 H_0^2 R}{\gamma} \tag{45}$$

is the magnetic Bond number

$$h = \frac{H}{H_0}, \quad h_n = \frac{H_n}{H_0}, \quad H_0 = \frac{m}{\delta^2}, \quad S_0 = 2\pi R^2, \tag{46}$$

$$h = \frac{1}{[1 + \sin^2\omega + (R/\delta)^2 + 2(R/\delta)\sin\theta\cos\phi - 2(R/\delta)\sin\omega\sin\theta]}, \tag{47}$$

$$h_n = \frac{R/\delta + \sin\theta\cos\phi + \sin\omega\cos\theta}{[1 + \sin^2\omega + (R/\delta)^2 + 2(R/\delta)\sin\theta\cos\phi - 2(R/\delta)\sin\omega\sin\theta]^{3/2}} \tag{48}$$

and $\mathrm{d}S = R^2 \sin\theta\, \mathrm{d}\theta\, \mathrm{d}\phi$. Due to the flow considered, the mean blood flow velocity $u_0$ does not enter into the adhesion condition (44), either directly through the viscous pressure (22)–(23), or indirectly through the hydrodynamic pressure (34)–(35). Placing the magnetic point source at $z = \zeta > 0$ ($\omega \neq 0$) (see Fig. 2(b)) results in a non-vanishing magnetic traction along the flow direction, that may balance the drag due to the blood flow. This traction balance can be expressed as an additional global condition, that results from the projection of Eq. (43) along the flow direction $\hat{\boldsymbol{e}}_z$ and the integration over the surface of the magnetic drop $S_1$:

$$\int\int_{S_1} (\llbracket T_z \rrbracket - p_c \hat{n}_z)\, \mathrm{d}S = 0. \tag{49}$$

The above condition can be interpreted as a way to take into account the deformation of the magnetic drop due to the blood flow (see Fig. 2(a)), that it is not included in the proposed solution. Provided that we can express this angle $\omega$ as a function of the drop deformation, the model becomes also quantitative and further detailed calculations of the flow need not be performed. In dimensionless form Eq. (49) reads

$$V_m = \frac{\chi}{2\beta S_0} \int\int_{S_1} [(h^2 - (1 + 2\chi)h_n^2)\hat{n}_z + 2\chi(1 + \chi))h_n h_z]\, \mathrm{d}S, \tag{50}$$

where

$$V_m = \frac{\eta_2 u_0}{\mu_0 H_0^2 R} \tag{51}$$

is the dimensionless velocity

$$\beta = \frac{\gamma_v - 1}{\gamma_v + 1}, \quad \gamma_v = \frac{\eta_2}{\eta_1}, \tag{52}$$

$$h_z = \frac{(r/\delta)\cos\theta - \sin\omega}{[1 + \sin^2\omega + (r/\delta)^2 + 2(r/\delta)\sin\theta\cos\phi - 2(r/\delta)\sin\omega\sin\theta]^{3/2}} \tag{53}$$

and $\hat{n}_z = \cos\theta$. Note that the capillary pressure does not enter the condition (50), resulting in the dimensionless velocity (51) with its limitations, due to the presence of the magnetic field. Thus instead of one adhesion condition (44), we now have two Eqs. (44) and (50) and the dependence of blood flow velocity on the applied magnetic field is parameterized as $B_m = B_m(R/\delta, \chi, \omega)$ and $V_m = V_m(R/\delta, \chi, \omega, \gamma_v)$. The obtained law $V_m = V_m(B_m)$ constitutes an upper bound to the correct one, since an additional constraint, Eq. (50) is introduced. Provided that a method can be devised that computes a lower bound close to the upper bound, the exact result may not need to be determined at all. Such a method, which will not be examined here, is to apply again the variational principle, that resulted to the field equations, after removing a positive term from the energy functional.

## 5. Results

The double integrals in Eqs. (44) and (50) can in some cases be obtained in closed analytical form but since they do not have any irregular behavior they can be computed numerically with high accuracy. The $\beta$ factor in Eq. (50), is susceptible of corrections, after computing a more accurate flow velocity field. The dependence of dimensionless velocity $V_m$ on the Bond number $B_m$ is very sensitive to parameter $(R/\delta, \chi, \omega, \gamma_v)$, variations. We are interested for realistic blood flows: a diluted ferrofluid ($\chi \ll 1$), bulk ($R \ll \delta$), and surface ($0 < R/\delta < 1$) vessels. The bulk vessels correspond mainly to arteries, while the surface vessels to veins. Angle $\omega$ was varied in the interval $0 \leqslant \omega \leqslant \pi/6$.

Results are presented in Figs. 3(a) and (b) after eliminating $\omega$, for varying viscosity ratio $\gamma_v$ and magnetic susceptibility $\chi$, respectively, and for two values of the ratio $R/\delta = 0, 0.2$. The curves intersect the Bond number axis for $\omega = 0$, as expected, since in this limiting case the present model fails to estimate the critical magnetic field for adhesion. In the case of bulk vessels ($R/\delta \ll 1$) the intersection with the $B_m$-axis corresponds to $B_m = 3/\chi$. For $\omega \geqslant \pi/6$ there is a maximum in the $V_m = V_m(B_m)$ curves, but these

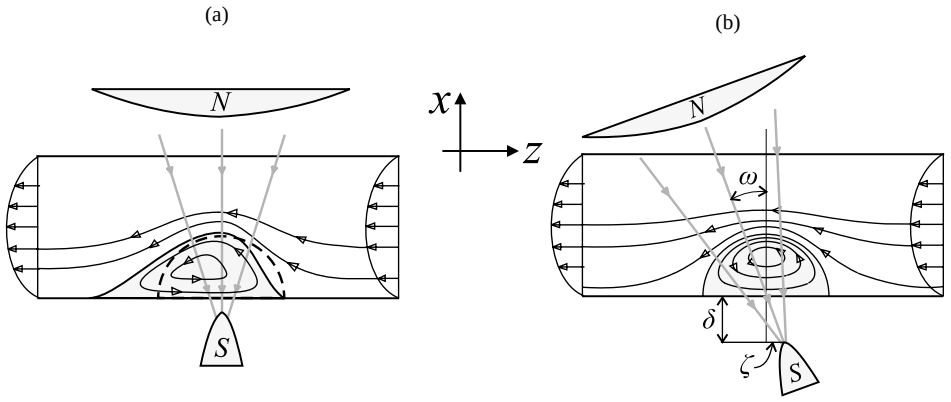


Fig. 2. The deformation of the magnetic drop (a) and its interpretation in the model (b).

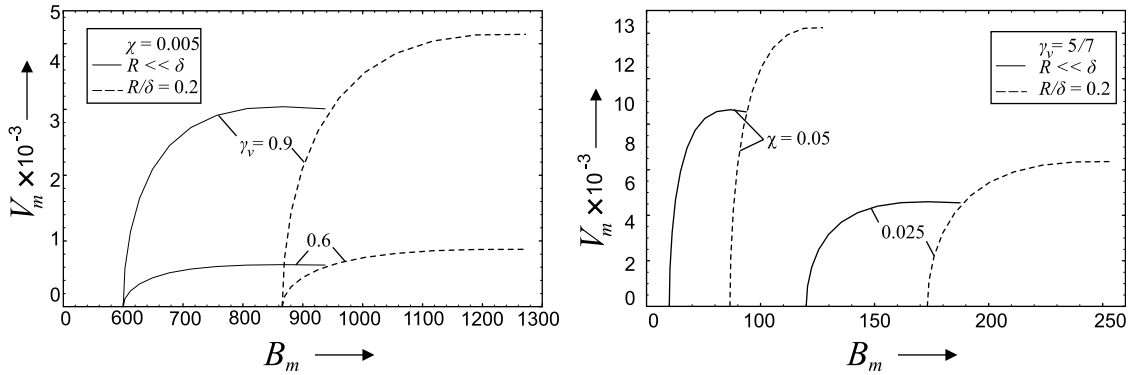


Fig. 3. Magnetic bond number $B_m$ vs. $V_m$, for (a) $\chi = 0.5$ and varying $\gamma_v$, (b) $\gamma_v = 0.5$ and varying $\chi$. Solid lines correspond to $R/\delta = 0$ and dashed to $R/\delta = 0.2$.

calculations are not shown, since they lead to physically unacceptable results. As expected (see Fig. 3(a)), higher ferrofluid viscosity (smaller $\gamma_v$) results, for the same magnetic field, to smaller blood flow velocities for adhesion. Examination of Figs. 3(a) and (b) might erroneously lead to the conclusion that for the same blood velocity it is needed higher magnetic field for smaller $\delta$ (see Fig. 3(a)) and $\chi$ (see Fig. 3(b)). This is not valid since the velocity becomes dimensionless by using the magnetic field, see Eq. (51) (the capillary pressure term vanishes in Eq. (49)).

In order to compare our results with available experimental data, we have also to compute and the magnetic force on the surface of the ferrofluidic drop. Due to the linearity of the magnetization-magnetic field law $M = \chi H_0$, the dimensionless mean magnetic force on the ferrofluid surface is given in terms of the parameters of Eqs. (46) and (47) as

$$f_m = \frac{2\chi}{S_0} \int \int_{S_1} h^{5/2} \, \mathrm{d}S \tag{54}$$

with

$$f_m \equiv \frac{F_m \delta}{\mu_0 H_0^2}. \tag{55}$$

Table 1

| | Units (SI) | Femoral artery ($R/\delta \approx 0$) | Carotid artery ($R/\delta = 0.2$) |
|---|---|---|---|
| $\omega$ | Degrees | 2.866 | 2.866 |
| $H_0$ | $T$ | 0.195 | 0.234 |
| $u_0$ | m/s | 0.462 | 0.841 |
| $u_{\exp}$ | m/s | 0.05–0.35 | 0.1–0.6 |
| $F_m$ | kN/m$^3$ | 5.992 | 105.025 |
| $\mathrm{d}H/\mathrm{d}x$ | T/m | 7.747 | 107.824 |
| $M$ | mT | 0.975 | 1.170 |
| $\delta$ | mm | 50 | 2.5 |

Alhough the present model is valid for low Reynolds number we summarize in Table 1, some results for bulk (femoral artery) and surface (carotid artery) veins. They correspond to a diluted magnetic drug with susceptibility $\chi = 0.005$, viscosity ratio $\gamma_v = 5/7$, surface tension $\gamma \approx \gamma_{\text{water}} = 25 \times 10^{-3}$ N/m, magnetic drop radius $R = 0.5$ mm and blood viscosity $\eta_2 \approx 3\,\eta_{\text{plasma}} = 6 \times 10^{-3}$ N s/m$^2$, in the expected range $\eta_{\text{blood}} \approx (1.58 - 3.8) \times 10^{-3}$ N s/m$^2$ come across the literature (Mokken et al., 1996; Dintenfass, 1968). The computed blood flow

velocities for adhesion are higher than the experimentally observed ones (Perret and Sloop, 2000), since the model computes an upper bound. The magnetic field $H_0$ and the magnetic force $F_m$ are in the expected range with similar experimental estimations, $0.1-0.7$ T and $3-150$ kN/m$^3$, respectively (Ruuge and Rusetski, 1993). The magnetic field gradient $\mathrm{d}H/\mathrm{d}x$ is calculated at $\boldsymbol{r}=(R,0,0)$ and is out of the experimentally estimated range $50-100$ T/m (Ruuge and Rusetski, 1993), due to the simplified Coulomb magnetic spike considered. The ferrofluid magnetization $M$ is also out of the experimentally estimated range $0.1-0.5$ mT, due to the linearity of the constitutive law.

Finally, the magnetic force–viscosity ratio relation ($f_m=f_m(\gamma_v)$) derived from our model is compared with experimental data from Fig. 6 of Ruuge and Rusetski (1993). For this purpose we interchange the parameters $\beta$ and $V_m$ in Eq. (50) and solve the resultant equation for $\gamma_v$, which gives

$$\gamma_v=\frac{1-\kappa}{1+\kappa} \tag{56}$$

with

$$\kappa=\frac{\chi}{2V_mS_0}\int\int_{S_1}[(h^2-(1+2\chi)h_n^2)\hat{n}_z+2\chi(1+\chi))h_nh_z]\,\mathrm{d}S. \tag{57}$$

Results are presented in Fig. 4. The value $\gamma_v=1$ corresponds to $\omega=0$. As expected $f_m$ is an increasing function of $\gamma_v$, since smaller viscosity of the ferrofluid, $\eta_1$, requires larger magnetic force for adhesion. Again we might erroneously conclude from Fig. 4 that for the same viscosity ratio, increase in the magnetic force requires increase in the blood velocity for adhesion. This inconsistency is also attributed to the use of the magnetic field, in order for the velocity to become dimensionless. The experimental data (open circles) correspond to a rate constant characterizing the washing away of the drop of ferrofluid from the blood vessel wall value, defined on Fig. 6 of Ruuge and Rusetski (1993), of 0.2. The best fit to the experimental data (curve 4 of Fig. 4) corresponds to $R/\delta=0.2$, $\delta=2.5$ mm, $\chi=0.005$, $H_0=0.177$ T, $\eta_2=5.58\times10^{-3}$ N s/m$^3$ and $u_0=6.756$ cm/s. Note that the experiments of Ruuge and Rusetski (1993) performed for one phase flow (ferrofluid), while our model assumes two phase flow (blood–ferrofluid). Nevertheless, since our theory has irregular behavior at $\omega=0$ ($\gamma_v=1$) the above assigned value for $\eta_2$ was considered efficient for fitting purposes.

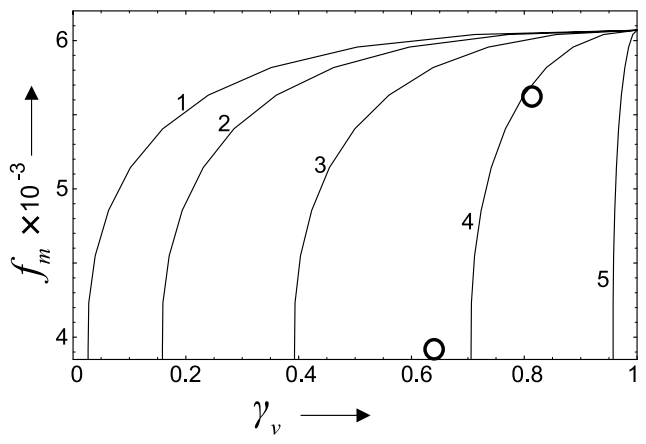


Fig. 4. Dimensionless magnetic force $f_m$ vs. $\gamma_v$ for varying $V_m$. Curves labeled 1–5 correspond to $V_m$ values 0.00023, 0.0003, 0.0005, 0.00126 and 0.01, respectively. The open circles are experimental data from Fig. 6 of Ruuge and Rusetski (1993).

## 6. Conclusions

The general theory for treating magnetic drug targeting, was developed. With minor corrections the theory can also be applied when the carrier is not a typical ferrofluid, but rather a lipid vessel (magnetoliposome). All necessary physical parameters like the strength and the orientation of the magnetic field, the magnetic composition of the drug, the blood composition and velocity are introduced in a model case. An upper bound to the critical magnetic field for magnetic drug capturing on blood vessel wall was derived. Provided that the orientation angle $\omega$, of the applied magnetic field will be related to the deformation and the diffusion of the drug, the model might become also quantitative. The difficulties on the design of proper non-uniform driving magnetic fields were discussed. The flexibility of the model permits the treatment of, either bulk (arteries), or surface (veins) blood vessels. The biocompatibility of the magnetic micro and nanobeads is a major issue and is imminently related to the possibility of biomineralization. Iron biomineralization processes have been observed in a variety of living organisms. Thus, it is expected that magnetite beads are more biocompatible compared to the more toxic nickel or cobalt oxides. It has to be addressed here, that at the final stages of a clinical application of such a process the presence of the magnetic drug in the targeting area depends mainly to the extent of the stenosis. It is expected though that such a process will not take place for more than 10–15 min and more over a suction instrumentation might be present, so biocompatibility is preserved even for more toxic ferrofluidics. Finally, in a long perspective, issues like the diffusion and dispersion of the drop through the porous vessel wall and in the blood stream, the pulsating character of the blood flow, the elasticity of the blood vessel, the phagocytosis of the magnetic drug (ferrofluid or magnetoliposome, in orgin), or the safety standards for magnetic fields, magnetic field gradients and the related exposure time intervals should also be investigated.

## References


Adrä, W., Nowak, H. (Eds.), 1998. Magnetism in Medicine, Wiley-VCH, New York.

Boudouvis, A., Scriven, L.E., 1993. Sensitivity analysis of the hysteresis in deformation of ferrofluid drops. Journal of Magnetism and Magnetic Materials 122, 254–258.

Dintenfass, L., 1968. Internal viscosity of the red cell and blood viscosity equation. Nature 219, 956–958.

Fung, Y.C., 1997. Biomechanics—Circulation, 2nd Edition. Springer Verlag, New York.

Haik, Y., Pai, V., Chen, C.J., 2001. Apparent viscosity of human blood in a high static magnetic field. Journal of Magnetism and Magnetic Materials 225, 180–186.

Higashi, T., Ashida, N., Takeuchi, T., 1997. Orientation of blood cells in static magnetic fields. Physica B 237-237, 616–620.

Iwasaka, M., Ueno, S., Tsuda, H., 1994a. Diamagnetic properties of fibrin and fibrinogen. IEEE Transactions on Magnetics 30, 4695–4697.

Iwasaka, M., Ueno, S., Tsuda, H., 1994b. Effects of magnetic fields on fibrinolysis. Journal of Applied Physics 75, 7162–7164.

Iwasaka, M., Ueno, S., Tsuda, H., 1996. Dissolution of thrombus under high gradient magnetic fields. IEEE Transactions on Magnetics 32, 5130–5132.

Iwasaka, M., Ueno, S., Tsuda, H., 1998. Polymerization and dissolution of fibrin under homogeneous magnetic fields. Journal of Applied Physics 83, 6453–6455.

Kilner, P.J, et al., 2000. Asymmetric redirection of flow through the heart. Nature 404, 759–761.

Kuznetsov, A, et al., 2001. Application of magnetic devices in otiatria. Journal of Magnetism and Magnetic Materials 225, 202–208.

Miller, M.M, et al., 2001. A DNA array sensor utilizing magnetic microbeads and magnetoelectronic detection. Journal of Magnetism and Magnetic Materials 225, 138–144.

Mosbach, K., Schröder, U., 1979. Preparation and application of magnetic polymers for targeting of drugs. FEBS Letters 102, 112–116.

Mokken, F.C, et al., 1996. Differences in peripheral arterial and venous hemorheological parameters. Annals of Hematology 73, 135–137.

Papathanasiou, A.G., Boudouvis, A., 1999. Three dimensional magnetohydrostatic instabilities of rotating ferrofluid drops. Journal of Magnetism and Magnetic Materials 201, 290–292.

Perret, R.S., Sloop, G.D., 2000. Increased peak blood velocity in association with elevated blood pressure. Ultrasound Medicine & Biology 26, 1387–1391.

Rosensweig, R.E., 1997. Ferrohydrodynamics. Dover Publications, New York.

Rusetski, A.N., Ruuge, E.K., 1990. Magnetic fluids as a possible drug carrier for thrombosis treatment. Journal of Magnetism and Magnetic Materials 85, 299–302.

Ruuge, E.K., Rusetski, A.N., 1993. Magnetic fluids as drug carriers: targeted transport of drugs by a magnetic field. Journal of Magnetism and Magnetic Materials 122, 335–339.

Schultheiss-Grassi, P.P, et al., 1999. TEM investigations of biogenic magnetite extracted from the human hippocampus. Biochemical and Biophysical Acta 1426, 212–216.

Torchilin, V.P., 2000. Drug targeting. European Journal of Pharmaceutical Science 11 (Suppl.), S81–S91.

Voltairas, P.A., Fotiadis, D.I., Massalas, C.V., 2001. Elastic stability of silicone ferrofluid internal tamponade (SFIT) in retinal detachment surgery. Journal of Magnetism and Magnetic Materials 225, 248–255.

Voustianiouk, A., Kaufmann, H., 2000. Magnetic fields and the central nervous system. Clinical Neuropysiology 111, 1934–1935.